Deformation monitoring of structural elements using terrestrial laser scanner

Zaki M. Zeidan[1] ,Ashraf A. Beshr[2], Ashraf G. shehata[3]
[1] Prof. of applied geodesy, Public Works department, Faculty of Engineering, Mansoura University,
zmze283@yahoo.com
[2] Ph.D., Assistant Prof., Public Works department, Faculty of Engineering, Mansoura University,
eng.aaabeshr@yahoo.com
[3] B. Sc., Demonstrator, Civil Engineering department, Delta University for Science and Technology,
ashrafgamal847@gmail.com

Abstract:

Civil infrastructure systems is important in terms of both safety and serviceability. So, large structure have been monitored using surveying techniques, while fine-scale monitoring of structural components has been done with geotechnical instrumentation. The advantages and disadvantages of using remote sensing methods, such as terrestrial laser scanning and digital close range photogrammetry, for the purposes of precise 3D reconstruction and the estimation of deflections in structural elements. This paper investigate that terrestrial laser scanner can be used for the monitoring of concrete beams subjected to different loading conditions. The system used does not require any physical targets. The setup was tested, and the beam deflections resulted from the 3D model from terrestrial laser scanner system were compared to the ones from ANSYS program. The experiments proved that it was possible to detect sub-millimeter level deformations given the used equipment and the geometry of the setup. Calculations and analysis of results are presented.

1. Introduction:

Health monitoring of infrastructure systems is an important task and is usually done for two reasons. The first one is safety (i.e. testing structural components or down-scaled models of designed structures in order to estimate their maximum loading capacity), and the second one is

serviceability (i.e. performing regularly scheduled monitoring procedures in order to assess whether any maintenance is required on an already built structure.[1]

Traditionally, large structures such as dams, bridges, open-pit mines or high-rise buildings have been monitored for overall deformations through ground based surveying techniques, i.e. measurement of horizontal angles (or directions), zenith angles, slope distances and height differences using precision grade total stations or theodolites and precision levels.

Recently, these techniques have been complemented by the use of global positioning methods, where geodetic grade receivers and antennas collect signals from all visible satellites in a static mode over long periods of time. [2].

Despite the wide variety of available surveying instruments and the well-established data processing and network adjustment techniques, they can only observe a limited number of points, which need to be carefully selected at the specific areas of anticipated deformation.

On the fine-scale side of structural health monitoring, the appearance of cracks and the failure of foundations, walls, support columns or structural components in general, have been measured via geotechnical techniques, for example using tilt meters, micrometers, inclinometers, wire strain gauges or extensometers. [3].

In order to avoid the above mentioned problems in large structure and in fine-scale deformation monitoring, remote sensing techniques can be used. In the last decade or so, sensors in the realm of digital photogrammetry and laser scanning have started to be integrated into structural health monitoring systems. The potential advantages of such remote sensing methods using cameras or laser scanners, are that the object of interest does not have to be accessed while being measured, and that permanent visual records (either images or point cloud scenes) of it are established for each observed epoch of time. [4]

Also, objects can be reconstructed and deformations can be detected in 3D with a great amount of redundancy, and the overall precision can be evaluated through a least squares adjustment. The monitoring of building structures have an increasingly important role in the engineering field, above all because they are concerned with the impact that such structures have in the area where they were built. Often, when walking through the old town centers, we realize just how obsolete and dangerous some buildings (even historic-cultural ones) are. The interest of some local governments in this problem has led, in the last few years, to the study and the trying out of measuring and monitoring methods which, quickly and at low cost, allow to define the extent of

the deformation and the degrade in an accurate and reliable way. [5] The most frequent cases of monitoring and control can be classified as follows: verification of the deformation and damage caused by natural calamities (e.g. earthquakes), or malicious (e.g. fires); verification of the de grade caused by weather conditions; verification of the present precarious state of a structure with respect to its initial project; verification of the result of bad workmanship. The requirement, therefore, is to identify techniques that are able to carry out accurate and reliable measuring of structural deformation, and that are easy to obtain and are not too expensive. Moreover, in case of the unstable buildings, especially if this are historic and cultural buildings, instruments are required that do not make direct contact with the structure itself. Among all the geomatic techniques, that have some of these characteristics, there are the following: measurement with Total Stations, measurement with GNSS technology, close range photogrammetry and Terrestrial Laser Scanning. [6]

one of studying the potential of Terrestrial Laser Scanning (TLS) in terms of monitoring structures and buildings that have been damaged by natural calamities or by malicious intent.

2. TERRESTRIAL LASER SCANNER (TLS):

The scanning of an object, or a building, consists of a series of scansions of the whole building, both internally and externally. The result obtained is a multitude of points which allow for a 3D reconstruction of the object with high accuracy.

FIG.1 Faro 3D laser scanner

The Faro 3D laser Focus (fig. 1). It is a compact scanner characterized by an operative range that varies between 0.6 m and 120 m with a linear distance error of ±2 mm for scanner object distances comprised between 10 m and 25 m, and a noise (that is to say, the standard deviation of the values with respect to the best-fit plan) which varies from between 0.6 mm and 10 mm with a reflectivity of 90% and 2.2 mm to 25 mm with a reflectivity of 10%. It has a vertical visual field of 305° and a horizontal one of 360°. The vertical and horizontal resolution is 0.009°. It has a scanning speed of 976.000 points/sec, and a reduced weight. Incorporated into the laser is a color digital camera with a resolution of 70 megapixels The laser scanning provides a point cloud with a high density points, each one of them having the coordinates x, y, z, relative to an intrinsic reference system to the instrument and the reflectivity, which is indicative of the physical characteristics of the surface scanned. [7]

3. Monitoring the structural deformation of reinforced concrete beam:

This section discusses an application of structural member monitoring. It presents a real time monitoring of a reinforced concrete simple beam subjected to specified concentrated loads. The three geodetic techniques have been applied to determine the values and directions of the actual deformations at specified sections and points under cases of loading. In deformation analysis, the functional relationship between the acting forces and the resulting deformations should be established. [8]

4. Experimental program:

The R.C beam have the section (300cm*30cm*30cm), and number of bars at upper and lower reinforcement, of them have 4Φ12 upper and the others have 4Φ16 lower, the steel used is high mild steel, the beam also have 5 Φ 8/m/ as stirrups. High Strength Concrete mix is used, the proposed mix is shown in table.

C	Ms/C	W/(C+Ms)	PZ	PZ/C	S	G/(S+G)	fc_7	fc_{28}
Kg/m^3	%		Type	%	Kg/m3		MPa	MPa
450	7	0.25	Conplast 430	3	650	0.65	41. 5	61. 0

Table .1 proposed mix of concrete beam

Where:

C= Cement, Ms= Micro silica, PZ= Super plasticizer, S= Sand, G=Gravel

Fc = 7, 28 days Cube Compressive Strength.

Composition of High Strength Concrete and selective mixture and Cube Compressive Strength Ordinary Portland cement and natural sand with high fineness modulus of 2.65 and Coarse aggregate (natural gravel) with a maximum of 12 mm are used. Powder silica fume with SiO2 of 92%, specific gravity of 2.2 and specific surface area of 16.8 m2/g is used. High Range Water Reducers super plasticizers) are used to improve both fresh and hardened concrete properties. The use of High Strength Concrete in the construction industry has steadily increased over the past years, which leads to the design of smaller sections. This is in turn reduces the dead weight, allowing longer spans and more area of buildings. High Strength Concrete has many applications as classical and non-classical applications. For these reasons, the High Reinforced Concrete is applied.

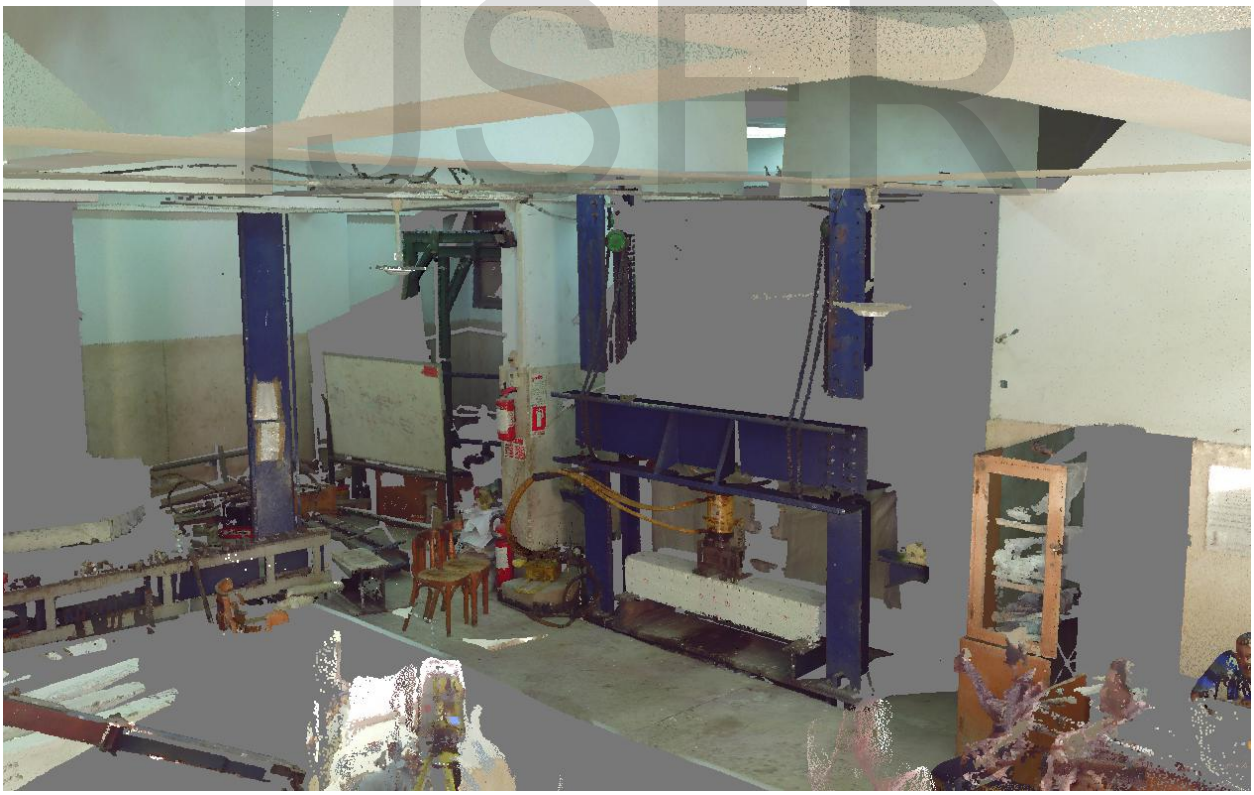

Fig.3 R.C Beam from TLS

5. Analysis of observations:

The beam is tested by using terrestrial laser scanner, the beam face is divided into 75 monitoring points. The spatial distribution of these points should provide complete coverage of the beam as shown in figure (4). A local three-dimensional rectangular coordinates system is needed to calculate the spatial coordinates of any monitoring point. Such a system, presumably, has Xaxis is chosen as a horizontal line parallel to the beam, the Y-axis is a horizontal line perpendicular to the base direction and positive in the direction towards the beam, the Z- axis is a vertical line determined by the vertical axis of the instrument.

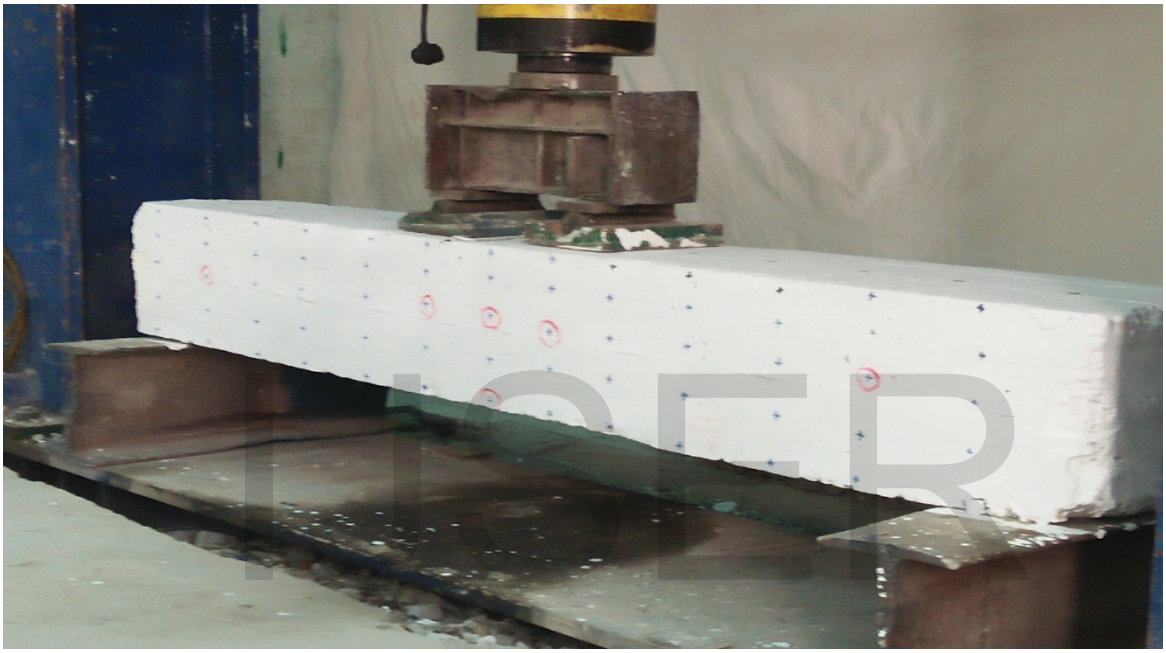

Fig (4) monitoring point on the beam

6. Executive Summary:

The main objective of this experiment is to monitor for deformations resulting from the loading test applied on 2 different beams material. (RC, Steel).

The scope of this document includes the results which will deliver reliable data prior to and after applying every load which will be compared with three different techniques.

7. Experimental work by using TLS:

The last beam is tested by using the terrestrial laser scanner technique, the beam face is divided into five critical monitoring points, and the spatial distribution of these points should provide

complete coverage of the beam. The selected monitoring points are located where the maximum deformations have been predicted such as point (**3)**, plus a few points which are depending on previous experience could signal any potential unpredictable behavior such as points (1, 2, 4 and 5).

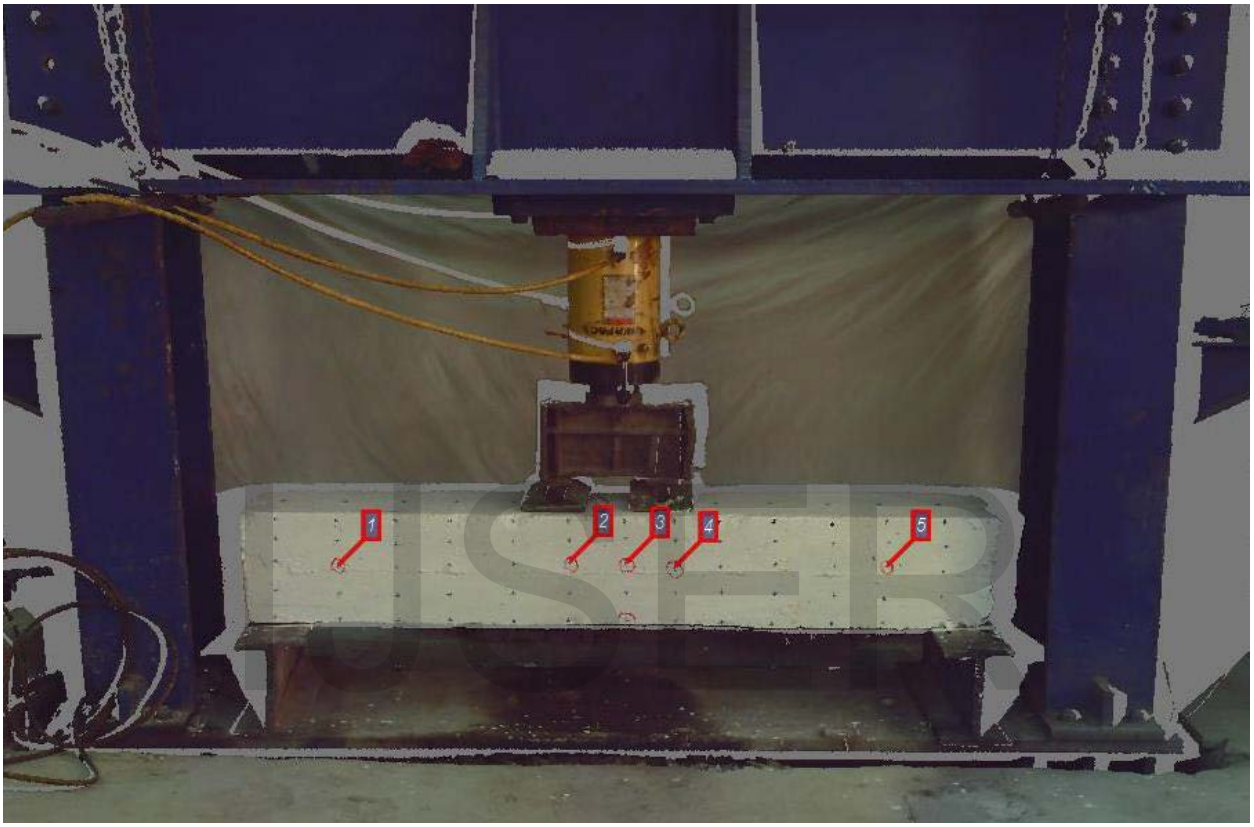

Fig (5) critical Points to be monitored with the RC Beam

The adjusted coordinates and its surveying accuracy of each monitoring point to the case of loading (0 ton) can be calculated. Table (2) shows a sample output of the adjusted coordinates (for Load **P** = 0 ton).

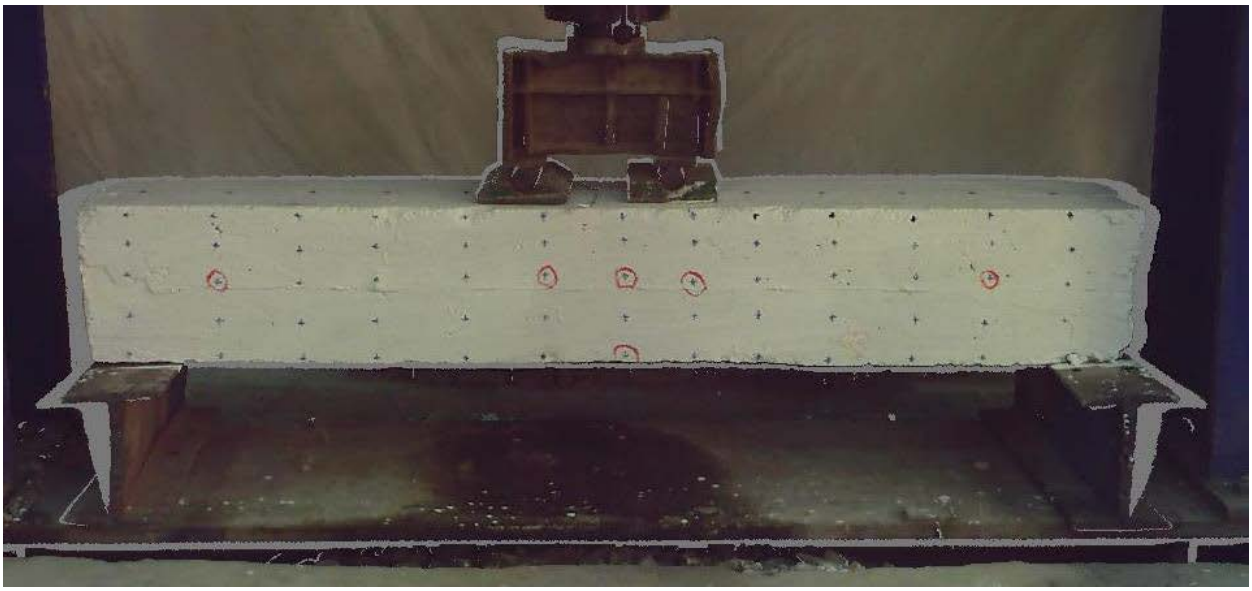

Fig (6) the RC beam in case of 0 ton load

Table (2) shows a sample output of the adjusted coordinates (for Load **P** = (0 ton)

point ID	Coordinates					
	X (m)	σX (mm)	Y(m)	σy (mm)	Z(m)	σz (mm)
1	-1.069	0.012	2.145	0.147	93.664	0.097
2	-0.455	0.124	2.239	0.216	93.677	0.028
3	-0.305	0.231	2.264	0.165	93.673	0.065
4	-0.175	0.021	2.285	0.187	93.661	0.032
5	0.386	0.178	2.378	0.098	93.664	0.014

Table (2) Adjusted coordinates of beam critical points and its accuracy (At P=0 ton)

The resulting surveying coordinates must be converted into meaningful engineering values. Point displacements in three dimensions are calculated by differencing the adjusted coordinates at each case of loading and the coordinates obtained at unload case.

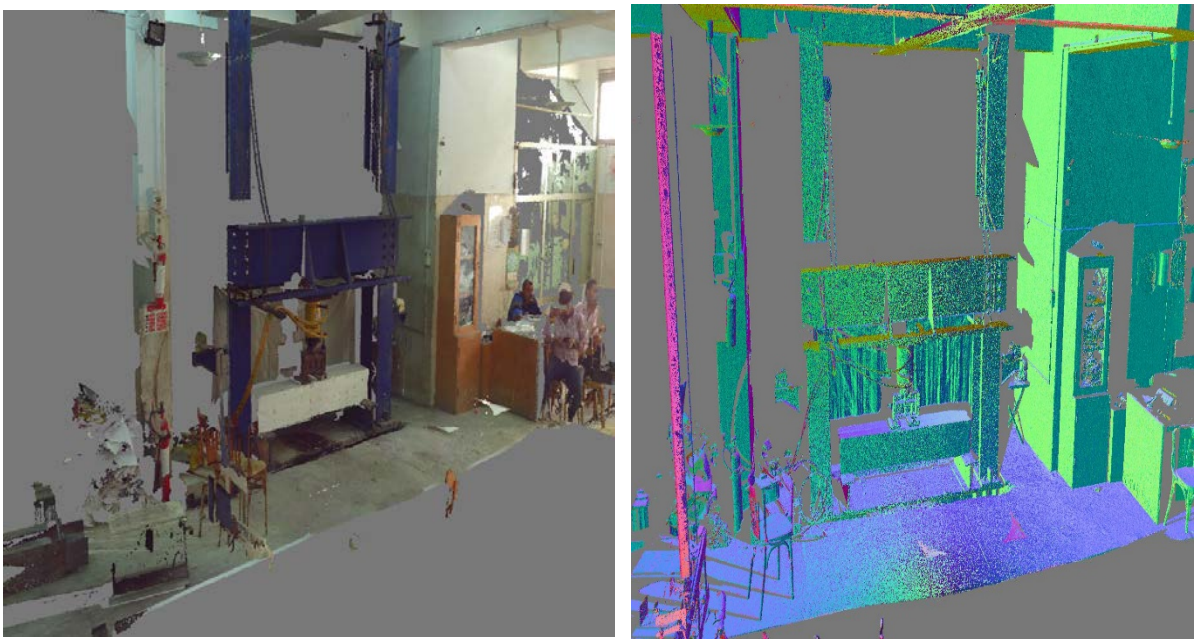

Fig (7) R.C beam from point cloud of TLS.

A comparison between the magnitudes of the calculated coordinate differences especially in **Z** direction for all loads with the UN loaded case.

point ID	Coordinates			difference from 0			difference from the previous load		
	X	Y	Z	ΔX	ΔY	ΔZ	ΔX	ΔY	ΔZ
1	-1.067	2.146	93.662	0.002	0.001	-0.002	0.002	0.001	-0.002
2	-0.454	2.241	93.676	0.001	0.002	-0.001	0.001	0.002	-0.001
3	-0.303	2.265	93.672	0.002	0.001	-0.001	0.002	0.001	-0.001
4	-0.176	2.288	93.66	-0.001	0.003	-0.001	-0.001	0.003	-0.001
5	0.387	2.378	93.665	0.001	0	0.001	0.001	0	0.001

A Comparison the magnitude of the calculated coordinate differences for load (5 ton)

point ID	Coordinates			difference from 0			difference from the previous load		
	X	Y	Z	ΔX	ΔY	ΔZ	ΔX	ΔY	ΔZ
1	-1.068	2.145	93.664	0.001	0	0	-0.001	-0.001	0.002

2	-0.455	2.241	93.674	0	0.002	-0.003	-0.001	0	-0.002
3	-0.304	2.263	93.671	0.001	-0.001	-0.002	-0.001	-0.002	-0.001
4	-0.177	2.286	93.658	-0.002	0.001	-0.003	-0.001	-0.002	-0.002
5	0.386	2.379	93.664	0	0.001	0	-0.001	0.001	-0.001

B Comparison the magnitude of the calculated coordinate differences for load (10 ton)

point ID	Coordinates			difference from 0			difference from the previous load		
	X	Y	Z	ΔX	ΔY	ΔZ	ΔX	ΔY	ΔZ
1	-1.067	2.143	93.66	0.002	-0.002	-0.004	0.001	-0.002	-0.004
2	-0.454	2.239	93.67	0.001	0	-0.007	0.001	-0.002	-0.004
3	-0.304	2.264	93.666	0.001	0	-0.007	0	0.001	-0.005
4	-0.175	2.286	93.655	0	0.001	-0.006	0.002	0	-0.003
5	0.386	2.379	93.661	0	0.001	-0.003	0	0	-0.003

C Comparison the magnitude of the calculated coordinate differences for load (15 ton)

point ID	Coordinates			difference from 0			difference from the previous load		
	X	Y	Z	ΔX	ΔY	ΔZ	ΔX	ΔY	ΔZ
1	-1.067	2.142	93.658	0.002	-0.003	-0.006	0	-0.001	-0.002
2	-0.453	2.24	93.663	0.002	0.001	-0.014	0.001	0.001	-0.007
3	-0.304	2.265	93.661	0.001	0.001	-0.012	0	0.001	-0.005
4	-0.176	2.285	93.648	-0.001	0	-0.013	-0.001	-0.001	-0.007
5	0.388	2.381	93.658	0.002	0.003	-0.006	0.002	0.002	-0.003

D Comparison the magnitude of the calculated coordinate differences for load (20 ton)

point ID	Coordinates			difference from 0			difference from the previous load		
	X	Y	Z	ΔX	ΔY	ΔZ	ΔX	ΔY	ΔZ
1	-1.069	2.141	93.655	0	-0.004	-0.009	-0.002	-0.001	-0.003

2	-0.455	2.24	93.652	0	0.001	-0.025	-0.002	0	-0.011
3	-0.303	2.264	93.647	0.002	0	-0.026	0.001	-0.001	-0.014
4	-0.173	2.287	93.635	0.002	0.002	-0.026	0.003	0.002	-0.013
5	0.388	2.379	93.653	0.002	0.001	-0.011	0	-0.002	-0.005

E Comparison the magnitude of the calculated coordinate differences for load (23 ton)

Table (3) Comparison the magnitude of the calculated coordinate differences for all loads

It is obvious that the displacements of points (1and 5) are less than the displacement of points (2, 3 and 4). The difference appears because of the rotation of the beam. The upper surface of the beam rotates more than the lower surface.

The max deformation for this beam from the initial coordinate at zero load and the final case of load (23 ton) is 26 mm at the mid span (point 3).

8. R.C beam deformation from software (ANSYS):

The analysis and behavior of normal and high strength concrete beams under axial load will be presented. This analysis predicts the behavior of system in elastic and post elastic stage, also drift at each story, stress and strain for both concrete and reinforcement, cracks propagation, bending, shear strength and deflection. The three dimensional nonlinear Finite element modeling of the system was performed using “ANSYS (15)” Program. In this model, the nonlinearity of concrete and reinforcement are considered. Concrete is modeled using a three dimensional reinforced concrete element named “SOLID”, which is capable of cracking in tension and crushing in compression. The main and web reinforcements are modeled using “STEEL” bar element within the concrete “SOLID” one.

Organization of this Clause included review on the material model for concrete and reinforcement, the input data (geometry, mesh data, loads, and boundary conditions), and finally discussed the behavior of system under load increasing.

9. Finite element model:

The finite element method using "ANSYS (15)" package can be used to closely predict the behavior of normal and high strength concrete beams under axial load. The load-deflection behavior, crack propagation, and first crack load, failure load and failure mode can be predicted using the finite element method with an accuracy that is acceptable for engineering purposes.

10. Meshing:

To obtain good results from the Solid element, the use of a rectangular mesh is recommended. Therefore, the mesh was set up such that square or rectangular elements were created (Figure 4.14). The volume sweep command was used to mesh the steel plate and support. This properly sets the width and length of elements in the plates to be consistent with the elements and nodes in the concrete portions of the model.

The necessary element divisions are noted. The meshing of the reinforcement is a special case compared to the volumes. No mesh of the reinforcement is needed because individual elements were created in the modeling through the nodes created by the mesh of the concrete volume. However, the necessary mesh attributes as described above need to be set before each section of the reinforcement is created.

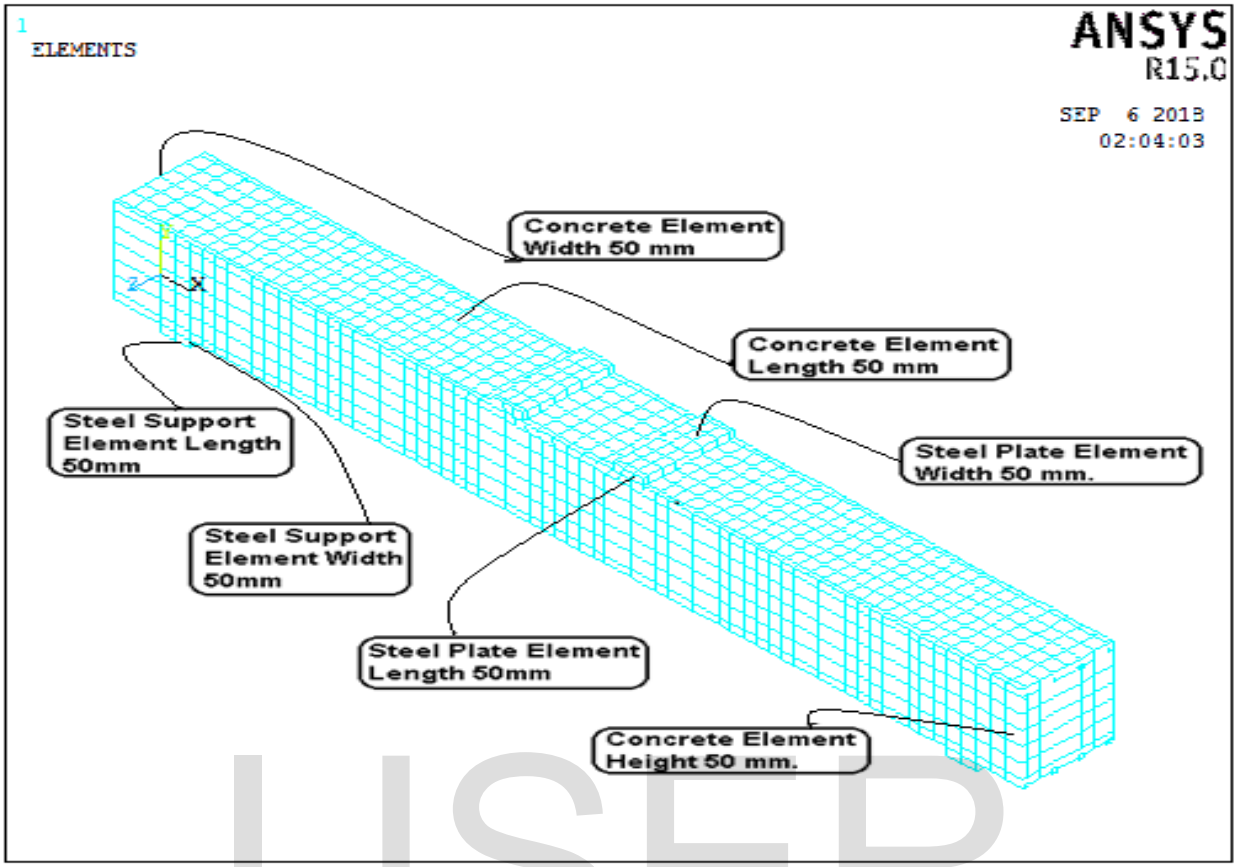

Fig (8) mesh from ANSYS

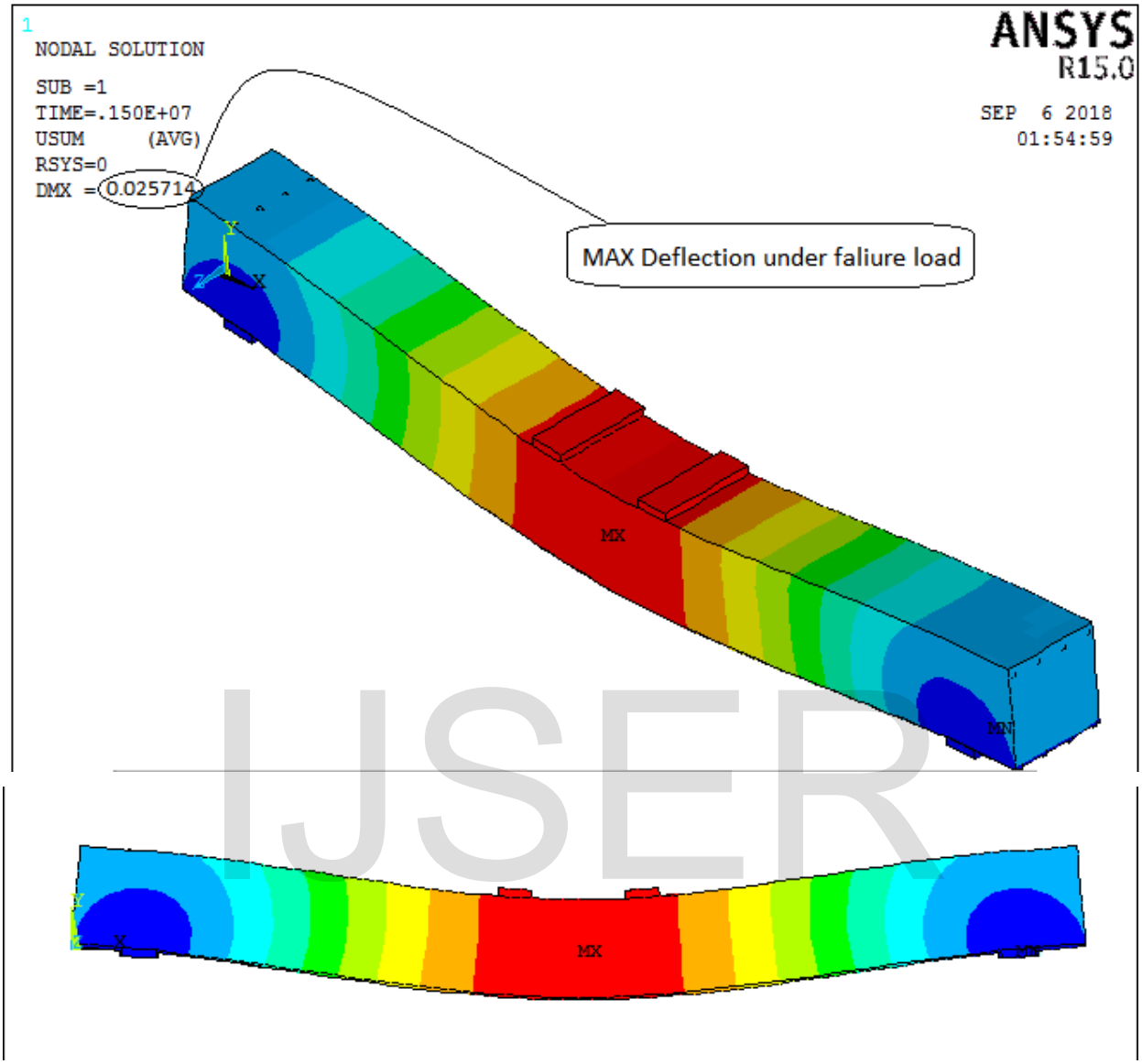

FIG (9) MAX Deflection from ANSYS program

The beam, plates, and supports were modeled as volumes. Since the beam is being modeled, the model is 3000mm. long, with a cross-section of 300*300mm. The zero values for the Z-coordinates coincide with the center of the cross-section for the concrete beam and the max deflection of the beam as shown in fig (9).

11. Comparison between TLS observations and other techniques:

load	δ (TLS)	δ ANSYS	l_2-l_1
0	0	0	0
5	0.002	0.001821	-0.0002
10	0.003	0.002672	-0.0003
15	0.007	0.006514	0.0002
20	0.014	0.013221	1E-04
23	0.026	0.025714	-0.0002

Table (4) Max deflection on concrete beam and difference between all techniques and TLS by using different instrument

The difference between observations are small the maximum difference 0.78 mm and the minimum difference 0.1 mm.

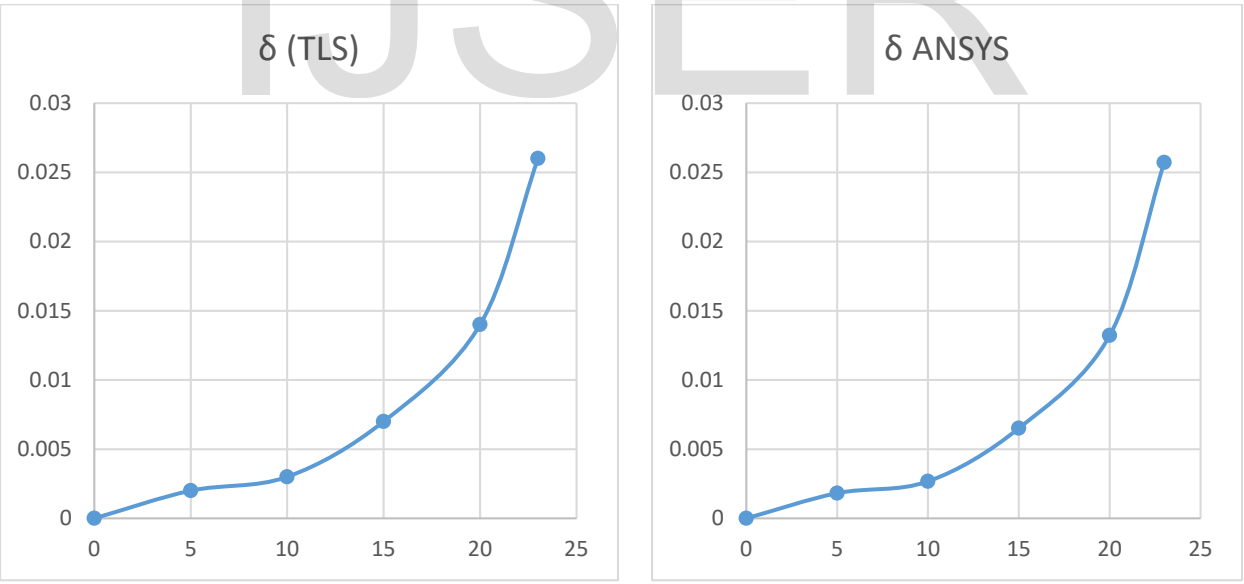

Fig (10) chart of max deflection for all technique

12. Experimental program for Steel beam:

The steel beam section is I beam 180 mm shown in fig (16)

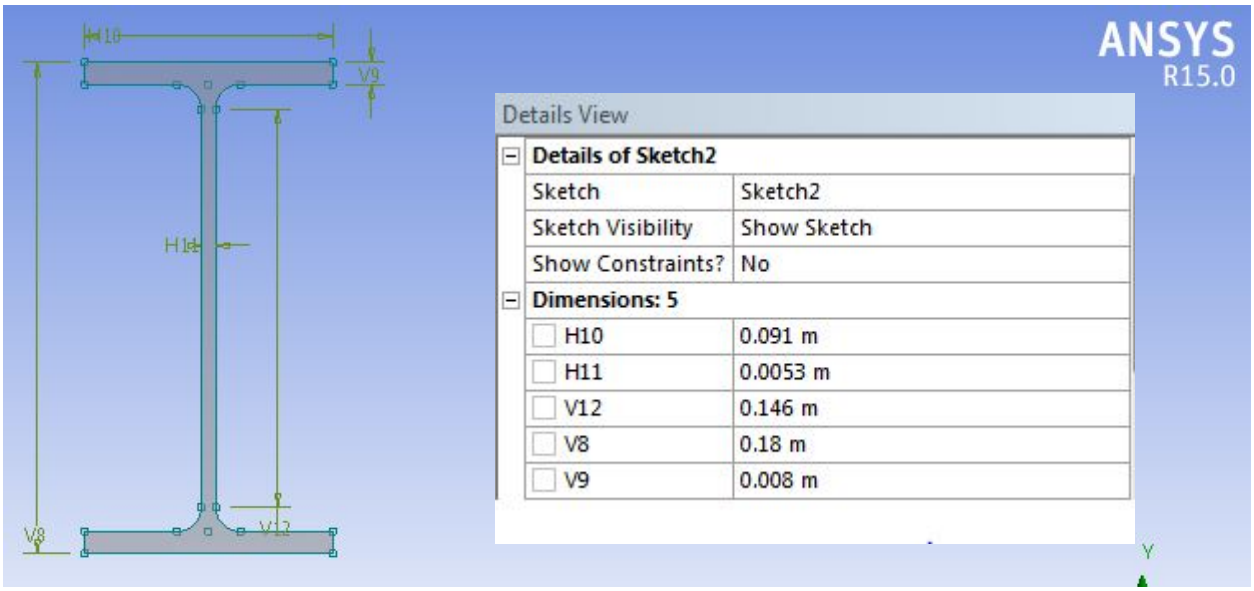

Fig (11) Steel I Beam dimensions

Fig (12) Steel Beam from TLS

13. Analysis of observations:

The beam is tested by using terrestrial laser scanner, the beam face is divided into 9 monitoring points. The spatial distribution of these points should provide complete coverage of the beam as shown in figure (13). A local three-dimensional rectangular coordinates system is needed to calculate the spatial coordinates of any monitoring point. Such a system, presumably, has X axis is chosen as a horizontal line parallel to the beam, the Y-axis is a horizontal line perpendicular to the base direction and positive in the direction towards the beam, the Z- axis is a vertical line determined by the vertical axis of the instrument.

Fig (13) monitoring point on the beam

14. Experimental work by using TLS:

The last beam is tested by using the terrestrial laser scanner technique, the beam face is divided into five critical monitoring points, and the spatial distribution of these points should provide complete coverage of the beam as shown in figure (14). The selected monitoring points are located where the maximum deformations have been predicted such as point (**3)**, plus a few points which are depending on previous experience could signal any potential unpredictable behavior such as points (1, 2, 4 and 5).

Fig (14) critical Points to be monitored with the RC Beam

The adjusted coordinates and its surveying accuracy of each monitoring point to the case of loading (0 ton) can be calculated. Table (5) shows a sample output of the adjusted coordinates (for Load **P** = 0 ton).

point ID	Coordinates					
	X (m)	σX (mm)	Y(m)	σy (mm)	Z(m)	σz (mm)
1	-1.069	0.012	2.145	0.147	93.664	0.097
2	-0.455	0.124	2.239	0.216	93.677	0.028
3	-0.305	0.231	2.264	0.165	93.673	0.065
4	-0.175	0.021	2.285	0.187	93.661	0.032
5	0.386	0.178	2.378	0.098	93.664	0.014

Table (5) Adjusted coordinates of beam critical points and its accuracy (At P=0 ton)

The resulting surveying coordinates must be converted into meaningful engineering values. Point displacements in three dimensions are calculated by differencing the adjusted coordinates at each case of loading and the coordinates obtained at unload case.

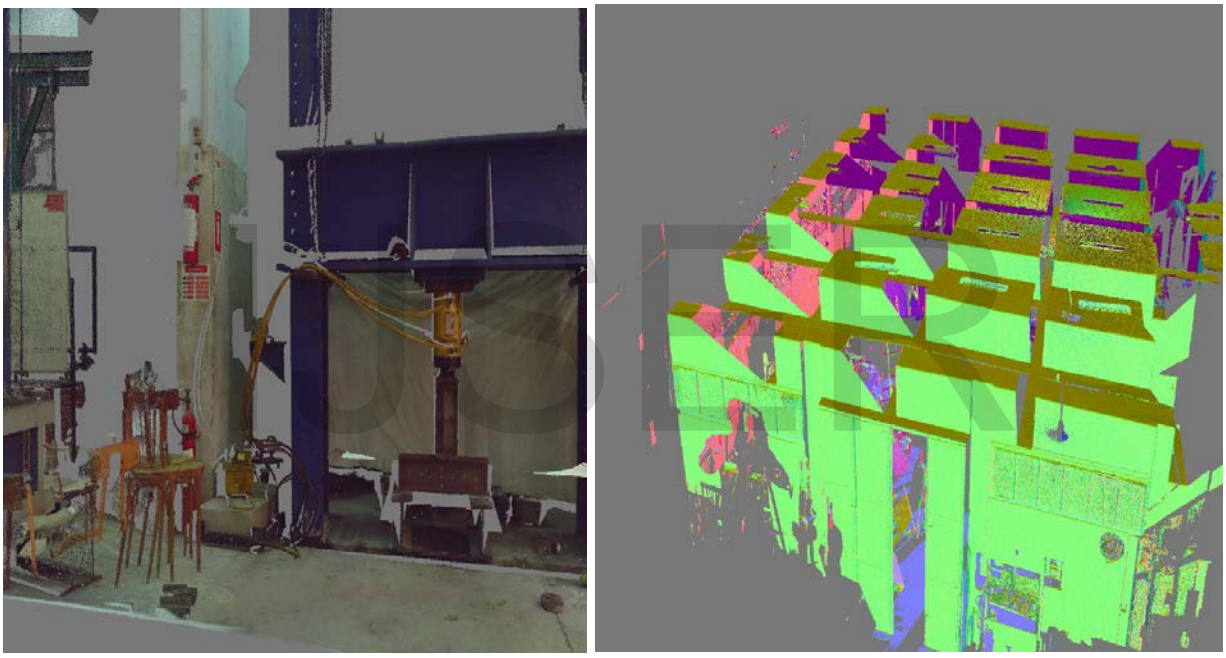

Fig (15) Steel beam from point cloud of TLS.

A comparison between the magnitudes of the calculated coordinate differences especially in **Z** direction for all loads with the UN loaded case.

point ID	coordinates			difference from 0			difference from the previous load		
	X	Y	Z	ΔX	ΔY	ΔZ	ΔX	ΔY	ΔZ
1	-0.698	2.325	93.589	0	-0.006	-0.004	0.001	0.005	0.002
2	-0.506	2.357	93.574	0.001	-0.009	-0.006	0.001	0.01	0.002
3	-0.409	2.37	93.577	0	-0.014	-0.008	-0.001	0.012	0.005
4	-0.309	2.389	93.577	0.002	-0.013	-0.008	-0.001	0.013	0.004
5	-0.109	2.432	93.577	0.001	-0.009	-0.002	-0.001	0.008	0

Table (6) Comparison the magnitude of the calculated coordinate differences for failure load

The vertical displacements at all loads and the failure load (P = 35 ton) is illustrated must be compared.

It is obvious that the displacements of points (1and 5) are less than the displacement of points (2, 3 and 4). The difference appears because of the rotation of the beam. The upper surface of the beam rotates more than the lower surface.

The max deformation for this beam from the initial coordinate at zero load and the final case of load (35 ton) is 8 mm at the mid span (point 3).

15. Steel beam deformation from software (ANSYS):

The analysis and behavior of normal and high strength concrete beams under axial load will be presented. This analysis predicts the behavior of system in elastic and post elastic stage, also drift at each story, stress and strain for both concrete and reinforcement, cracks propagation, bending, shear strength and deflection. The three dimensional nonlinear Finite element modeling of the system was performed using “ANSYS (15)” Program. In this model, modeled using “STEEL”.

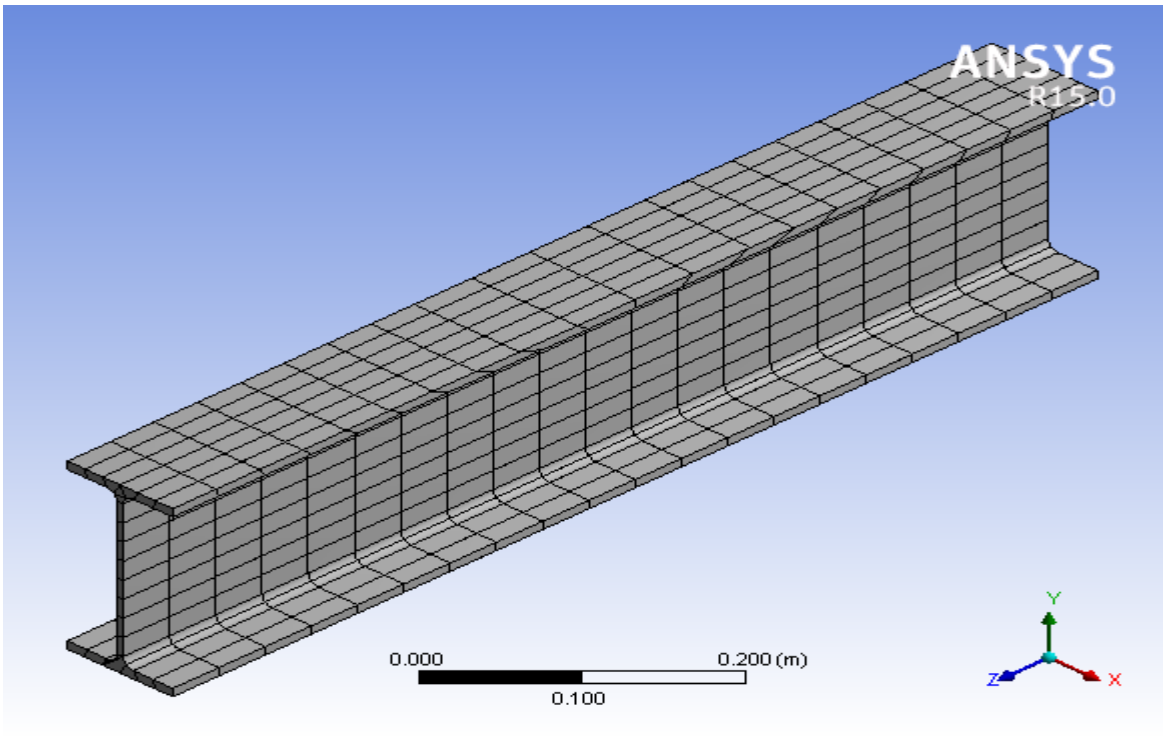

Fig (16) mesh from ANSYS

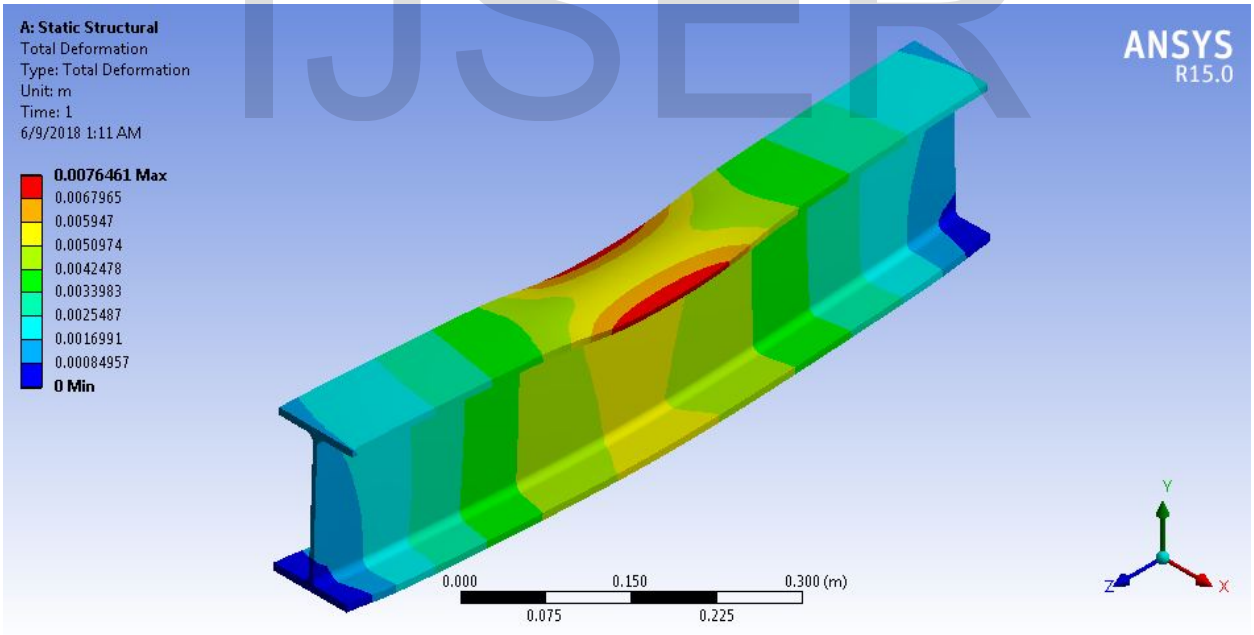

FIG (17) MAX Deflection from ANSYS program

16. Comparison between TLS observations and other techniques:

load	δ (TLS)	δ ANSYS	l_2-l_1
0	0	0	0
10	0.004	0.003788	-0.00021
30	0.008	0.007646	-0.00035

Table (6) Max deflection and difference between all techniques and TLS on steel beam

The difference between observations are small the maximum difference 0.35 mm and the minimum difference 0.2 mm.

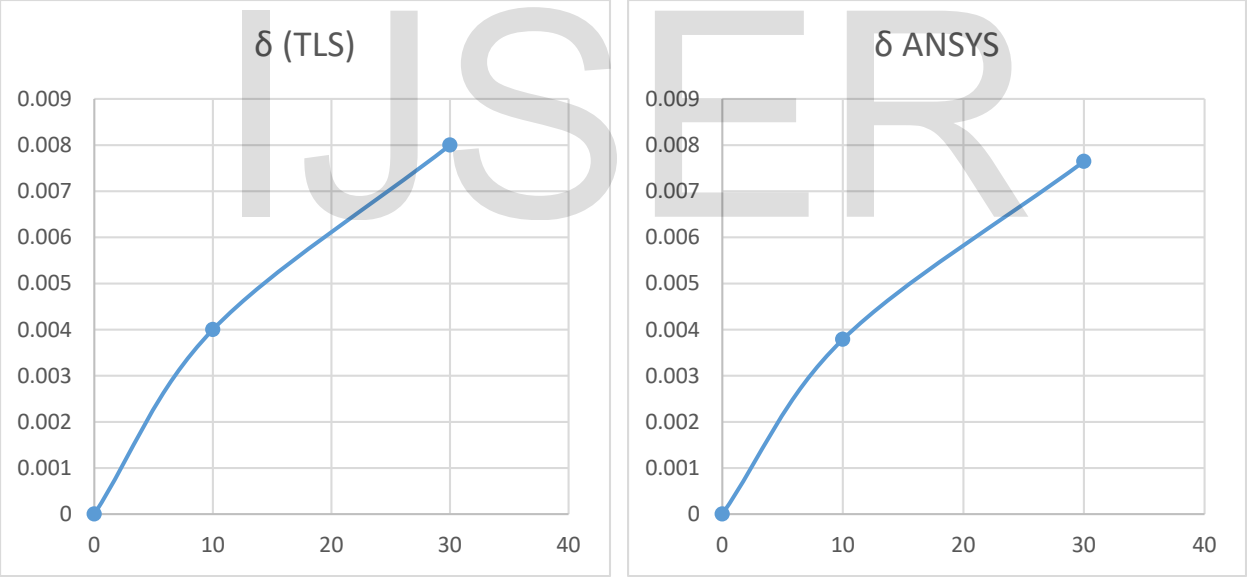

Fig (18) chart of max deflection for all technique

17. Conclusion:

1. TLS is a very fast acquisition method and does not require deployment of any targets on the object. Since the measurements are carried out touchless the performance and accuracy of the measurements depend on the surface properties of the object.
2. The max deformation for R.C beam from the initial coordinate at zero load and the final case of load (23 ton) is 26 mm at the mid span (point 3).
3. The max deformation for steel beam from the initial coordinate at zero load and the final case of load (35 ton) is 8mm at the mid span (point 3).
4. TLS is considered as valuable tool for monitoring the structure elements deformation with sufficient accuracy. It has also the ability to create 3D models of monitored object through loading.
5. Using TLS is better than any other geometric instrument for monitor the structure elements because its capability to draw and compare 3D model of element according to loading.
6. For R.C beam the maximum deformation from TLS observation (26 mm) and the maximum difference between TLS and other technology (0.78 mm) and the minimum difference (0.1 mm).
7. For steel beam the maximum deformation from TLS observation (8 mm) and the maximum difference between TLS and other technology (0.35 mm) and the minimum difference (0.2 mm).

18. Acknowledgment:

It was our honor to deal with very helpful company (micro engineering technology in Egypt). Thanks for all staff members for helping in the experimental works and field observations collection data.

19. Reference:

1. Bond et al., (2008)”system and method for remote asset monitoring” worldtelemetry inc.

2. I. Detchev a,*, A. Habib a, M. El-Badry b, (2011)" ESTIMATION OF VERTICAL DEFLECTIONS IN CONCRETE BEAMS THROUGH DIGITAL CLOSE RANGE PHOTOGRAMMETRY" International Archives of the Photogrammetry, Remote Sensing and Spatial Information Sciences.
3. I. Detchev a,*, A. Habib a, M. El-Badry b, (2014)" DEFORMATION MONITORING WITH OFF-THE-SHELF DIGITAL CAMERAS FOR CIVIL ENGINEERING FATIGUE TESTING" International Archives of the Photogrammetry, Remote Sensing and Spatial Information Sciences.
4. I. Wilczyńska, K. Ćmielewski, (2016)" Modern measurements techniques in structural monitoring on example of ceiling beams" Wroclaw University of Environmental and Life Sciences, Wroclaw, Poland.
5. K. L. El-Ashmawy, (2015)"A comparison between analytical aerial photogrammetry, laser scanning, total station and global positioning system surveys for generation of digital terrain model," Geocarto International.
6. Morteza Daneshmand et al , (2018) " 3D Scanning: A Comprehensive Survey " arXiv:1801.08863v1 [cs.CV].
7. park, richard d. miller, jianghai xia, and julian ivanov, (2007) "multichannel analysis of surface waves (masw)—active and passive methods" kansas geological survey, lawrence, usa.
8. S. El-Omari and O. Moselhi, (2008)"Integrating 3d laser scanning and photogrammetry for progress measurement of construction work, "Automation in construction.